SDSS'Rio 2010 STABILITY AND DUCTILITY OF STEEL STRUCTURES
E. Batista, P. Vellasco, L. de Lima (Eds.)
Rio de Janeiro, Brazil, September 8 - 10, 2010

EXPERIMENTAL STUDY ON COLD-FORMED STEEL LIPPED CHANNEL COLUMNS UNDERGOING LOCAL-DISTORTIONAL-GLOBAL INTERACTION

Eliane S. Santos*, Eduardo M. Batista* and Dinar Camotim**

*Civil Engineering Program, COPPE, Federal University of Rio de Janeiro, Brazil
e-mails: elianesantos@coc.ufrj.br, batista@coc.ufrj.br

**Department of Civil Engineering, ICIST/IST, Technical University of Lisbon, Portugal
e-mail: dcamotim@civil.ist.utl.br

Keywords: Cold-formed steel columns, Lipped channels, Local-distortional-global interaction, Ultimate strength, Experimental analysis.

Abstract. *This paper reports the available results of an ongoing experimental investigation on fixed cold-formed steel lipped channel columns undergoing local-distortional-global mode interaction, i.e., exhibiting nearly coincident local, distortional and global (flexural-torsional) critical buckling loads. After addressing the preliminary buckling analyses, performed to select appropriate column geometries (cross-section dimensions and lengths), a detailed description of the experimental program carried out at COPPE/UFRJ is provided. Next, the most relevant experimental results obtained during the tests are presented and discussed. Finally, the paper closes with some considerations concerning the design of the columns investigated in this work – in particular, the application of the design expressions currently prescribed by the Direct Strength Method is assessed.*

1 INTRODUCTION

Due to their high wall and overall slenderness, cold-formed steel members are highly susceptible to several instability phenomena, namely to buckling in local (*L*), distortional (*D*) or global (*G* – flexural, torsional or flexural-torsional) modes. For some particular (but of practical interest) combination of member cross-section geometry (*i.e.*, shape and dimensions) and length, the critical stresses associated with two or three of the above buckling modes coincide, thus leading to the occurrence of *mode interaction* phenomena, which may have a detrimental effect on the member strength. Depending on the buckling modes involved, one may be faced with *L-D*, *L-G*, *D-G* or *L-D-G* interaction. Because distortional buckling was not unveiled and properly understood until about two decades ago, for quite a long time *L-G* was the only type of mode interaction widely acknowledged and investigated, both analytically and experimentally, by the cold-formed steel community. As a result, reliable design rules and recommendations were continuously developed, improved and included in codes of practice – *e.g.*, in the current versions of the North-American [1] and Brazilian [2] specification for the design of cold-formed steel structures. Concerning the *L-D* interaction, it has been recently shown (*e.g.*, [3-5]) that it may lead to a significant strength erosion, which may be handled by means of an approach based on the Direct Strength Method (DSM – *e.g.*, [6]). Although the *D-G* interaction was already addressed by Dinis and Camotim [7], most of the current research effort has been devoted to the *L-D-G* interaction – the focus of the work presented in this paper. The available results of the investigation currently under way have already been reported by Dinis and Camotim [8], Dinis *et al.* [9] and Santos [10].

The aim of this paper is to report the available results of an ongoing experimental investigation on the behaviour and design of fixed cold-formed steel lipped channel columns experiencing local-distortional-global mode interaction, *i.e.*, exhibiting coincident (or vey close) local, distortional and global (flexural-torsional) critical buckling loads. Initially, one addresses the preliminary buckling analyses, performed by means of analyses based on Generalised Beam Theory (GBT) and intended to select appropriate column geometries (cross-section dimensions and lengths). Then, the paper includes a detailed description of the experimental program carried out at

COPPE/UFRJ – special attention is paid to the column end support conditions, the specimen positioning and loading procedure, and the measurement of the initial geometrical imperfections and load-induced displacements. Next, the most relevant experimental results obtained during the tests are presented and discussed – they include column deformed configurations, collapse mechanisms, displacement profiles and equilibrium paths associated with the key displacements. Finally, the paper closes with some considerations on the design of lipped channel undergoing local-distortional-global interaction. In particular, one presents an experimental assessment of the application of the design expressions currently prescribed by the Direct Strength Method for global failures and collapses due to local-global interaction. A few concluding remarks/recommendations are made at the end.

2 PRELIMINARY BUCKLING ANALYSIS

In order to identify geometries (cross-section dimensions and length) of fixed lipped channel columns that are strongly affected by *L-D-G* interaction, *i.e.*, with coincident or near coincident local, distortional and global (flexural-torsional) critical buckling loads ($P_{cr.L} \approx P_{cr.D} \approx P_{cr.G}$), it was necessary to perform preliminary elastic buckling analyses. This task was carried out by means of the code GBTUL [11], which is based on Generalised Beam Theory (GBT) and, therefore, makes it possible also to obtain the variation of the critical load with the column length (L) and the corresponding modal participation diagram.

The GBT-based buckling analysis led to the identification of the four column geometries (web width b_w, flange width b_f, stiffener width b_s, length L and wall thickness t) given in table 1, for which the first three buckling loads, corresponding to local (several half-waves), distortional (a few half-waves) and global (one half-wave) buckling modes, are less than *3%* apart. Table 1 also includes the values of the above three buckling loads and the tested specimen designations[1], which will be addressed in the next section, when the experimental program is described.

Table 1: Nominal geometries and designations of the four column specimens affected by strong *L-D-G* interaction.

Column specimens	b_w (mm)	b_f (mm)	b_s (mm)	L (mm)	t (mm)	$P_{cr.L}$ (kN)	$P_{cr.D}$ (kN)	$P_{cr.G}$ (kN)
C1-3	81	78	12	2850	1.11	43.8	42.9	44.1
C4-6	75	65	11	2350	1.11	48.8	47.5	48.6
C7-8	71	60	11	2100	1.11	51.9	51.8	51.9
C9-10	62	55	11	1650	1.11	60.1	58.8	59.5

To illustrate the buckling results obtained, figures 1(a)-(b) show the curve P_{cr} *vs.* L (logarithmic scale) and a part of the modal participation diagram for the cross-section dimensions of the C4-6 tested specimens (see table 1) and the steel material properties $E=200\,GPa$ and $\nu=0.3$. The observation of these buckling results shows that:

(i) The column length range can be divided into three intervals, associated with different critical buckling mode natures: (i) I (shorter columns – $L<2045\,mm$), corresponding to *local* buckling and in which the P_{cr} *vs.* L curve descends monotonically up to $L\approx70mm$, before turning into an almost horizontal "plateau"; (ii) II (intermediate columns – $2045<L<2411\,mm$), associated with *distortional* buckling (*1-2* half-waves) and in which the P_{cr} *vs.* L curve descends slightly; and (iii) III (longer columns – $L>2411\,mm$), associated with *global* buckling modes (*1* half-wave) and in which the P_{cr} *vs.* L curve descends sharply.

(ii) The selected column length is $L=2350\,mm$ and falls inside interval II (but barely – see fig. 1(b)), which means that the column critical buckling load ($P_{cr}=47.5\,kN$) corresponds to *distortional* buckling. The second and third bifurcation loads, which are very close (less than *3%* – $P_{b2}=48.6\,kN$ and $P_{b3}=48.8\,kN$) are associated with *global* and *local* buckling, respectively.

[1] The dimensions included in table 1 are nominal values. Nevertheless, as will be commented in the next section, the measured dimensions of the tested specimens were found to be very close to the indicated nominal ones.

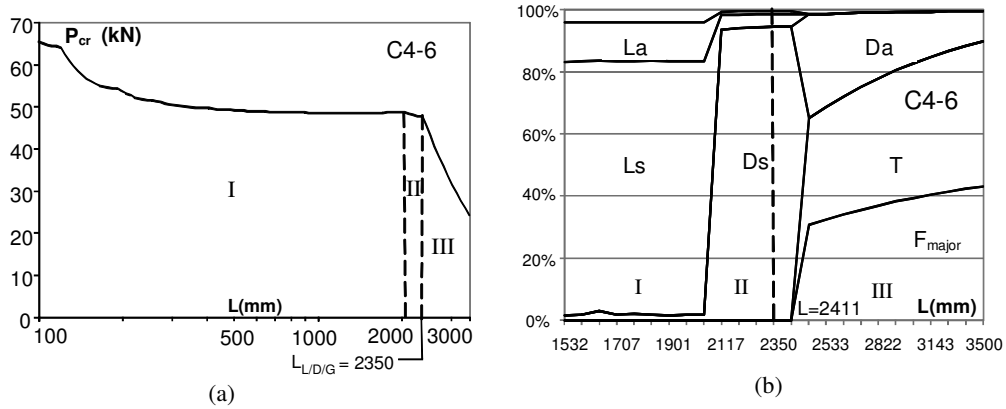

Figure 1: (a) Variation of the critical buckling load with the column length (logarithmic scale) and (b) part of the modal participation diagram (cross-section dimensions of specimens C4-6, $E=200\,GPa$ and $\nu=0.3$).

(iii) The part of the column modal participation diagram displayed in figure 1(b) provides relevant information on the variation of the critical buckling mode nature in the vicinity of the selected length value ($L=2350\,mm$). For the shorter lengths, corresponding to interval I, one has web-triggered local buckling combining about *80%* and *20%* of symmetric and anti-symmetric local deformation modes – for $L=2350\,mm$, this buckling mode is associated with P_{b3}. In the very close vicinity of $L=2350\,mm$, corresponding to interval II, the critical buckling mode is almost "pure distortional", as it combines a *95%* contribution of the symmetric distortional deformation mode with a tiny participation of the anti-symmetric local one. Finally, the longer columns, corresponding to interval III, buckle in modes that combines major axis flexure, torsion and anti-symmetric distortion (the contribution of the anti-symmetric distortional deformation mode decreases with the length, being "replaced" by higher contributions of the flexural and torsional modes)[2] – for $L=2350\,mm$, this "global" buckling mode is associated with P_{b2}.

3 EXPERIMENTAL PROGRAM

The column specimens were manufactured from high strength ASTM A572 steel of grade 50, which has a nominal yield stress equal to $f_y=345\,MPa$. Its mechanical properties were carachterised by means of standard tensile coupon tests, which made it possible to obtain the following mesured value ranges: (i) Young's modulus E varying from *205* to *216 GPa* and (ii) yield stress and tensile strength average values of $f_y=342\,MPa$ (standard deviation of *1.2%*) and $f_u=439\,MPa$ (standard deviation of *4.1%*), respectively. The column cross-section dimensions were measured at five different locations along the length and the values obtained are fairly identical to the nominal ones indicated in table 1 (standard deviation below *1%* and maximum difference of *5%*). Concerning the wall thickness, the measured values varied from *1.05* to *1.09 mm*, i.e., slightly below the nominal value *1.11 mm*. Moreover, the angle formed by the web and flange wall elements was also measured (at least 4 measuements for each specimen) – the average value found was *1.577 rad* (*90.364°*), with a standard deviation of *1.61%*.

In order to guarantee that the specimen end cross-sections were effectiely fixed, they were welded (TIG welding) to *12 mm* thick steel plates that were connected to the testing frame loading plates by means of four *10 mm* diameter bolts – a view of the column end support conditons is depicted in figure 2. The testing frame loading plates are connected to spherical hinges, which (i) are free to rotate during the positioning of the column specimen, prior to

[2] Note that the so-called column "global" buckling mode is, indeed, a flexural-torsional-distortional one. The presence of the anti-symmetric dimensional deformation mode, which already unveiled in [8,9], has significant implications in the column post-buckling behaviour.

the test, and and (ii) are fully restrained against rotations, during the test. Concentric axial loading was ensured by (i) preliminary measurements that enable an accurate positioning of the end cross-sections on the end plates, before welding, and (ii) the centering of the end plate on the test frame loading plate, with the help of the free-to-rotate spherical hinges. Therefore, it is fair to say that there are minute (negligible) eccentricities of the end section centroids with respect the test frame loading axis.

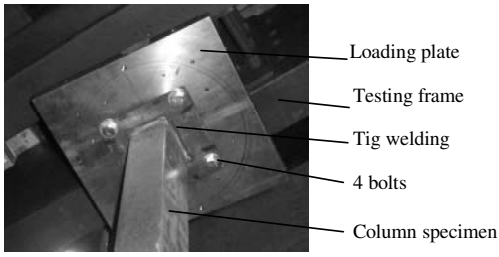

Figure 2: Column end cross-section fully fixed against the test frame loading plate.

The column initial geometrical imperfections and load-induced displacement were measured with the help of *8* displacement transducers (DT1 to DT8), located around the column cross-section as indicated in figure 3(a) – this figure also includes the sign convention adopted for the measured displacements. Three of these displacement transducers (DT6, DT7 and DT8) are mounted on a device that is able to move along the whole column length – its position (along the column length) is monitored by means of an additional displacement transducer DT9. The remaining *5* dispacement transducers were always located at the column mid-height. Figure 3(b) shows a view of the positioning of the various displacement transducers at the column mid-height.

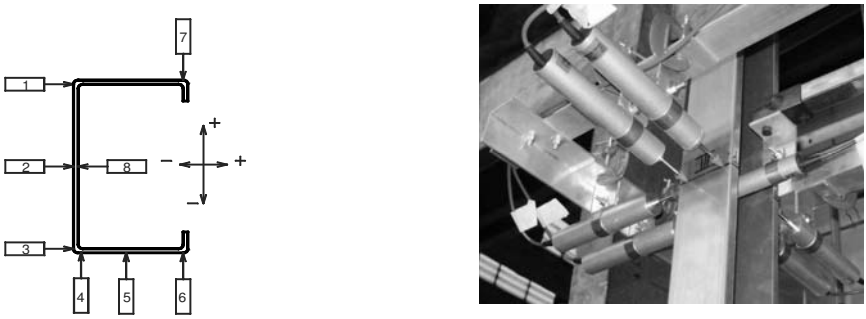

Figure 3: (a) Position of the displacement transducers around the column cross-section and displcement sign convention, and (b) view of the displacement transducer positioning at the column mid-height.

Concerning the measurement of the initial geometrical imperfections, it (i) was made after having properly positioned the column specimen in the testing frame and (ii) involved single (mid-height) measurements from the *5* fixed displacement transducers and continuous measurements from the three ones mounted on the moving device. During the load application, all displacement transducers remained fixed at the column mid-height and their readings were continuously fed into a data acquisition system, making it possible to plot several load-dispalcement equilibrium paths, namely those associated with flexural or distortional lateral displacements and torsional rotations. Moreover, at selected load values, the loading process was interrupted and the device with the displacement transducers DT6, DT7 and DT8 was moved along the column length, in order to try to obtain experimental evidence of the occurrence of local (DT8) and/or symmetric distortional (DT6 and DT7) deformations in the columns.

Finally, it is worth mentioning that the compressive loading system was set to a displacement control mode and that the accuracy of the loading measured and fed to the data acquisition system was *50 N*.

4 EXPERIMENTAL RESULTS

This section reports the main experimental results obtained from the performance of *10* tests, concerning the column specimens indicated in table 1, all of which were selected to exhibit coincident (or, at least, as close as possible) local, distortional and global critical buckling loads ($P_{cr.L} \approx P_{cr.D} \approx P_{cr.G}$). Due to both space limitations and the fact that the various tests provided qualitatively similar outputs, only the experimental results concerning the tested specimen C4 (see table 1) are presented here – the interested reader may find the complete set of experimental results in reference [10]. After the performance of all the tests and the close observation of the results obtained, the following conclusions may be drawn (they are valid for all the columns tested):

(i) In the early loading stages (elastic range), all the columns exhibited a clearly visible flexural-torsional deformed configuration, as illustrated in figure 4(a).

(ii) All the columns developed the plastic collapse mechanism depicted in figure 4(b), which consists of the formation of a mid-height "local plastic hinge" typical of slender plates. When failure occurred, the column (largely) deformed configuration was clearly flexural-torsional.

(iii) The displacement profiles obtained from the measurements of the displacement transducer DT8 at four load levels (P_{exp}=*0.6-9.0-23.7-28.3 kN*) are displayed in figure 5. Although these displacement profiles are fairly "irregular", making it quite difficult to assess whether or not local deformations take place, the visual inspection of the column during the test did not detect any sign of local deformations.

(iv) The displacements profiles obtained from the measurements of the displacement transducers DT6 and DT7 at two load levels (P_{exp}=*0.6-28.3 kN* – initial and final loading steps) are depicted in figure 6. Figure 7, on the other hand, shows the equilibrium paths concerning displacements recorded by these two transducers at the mid-height cross-section. Since the presence of symmetric distortional deformations is associated with the difference between the DT6 and DT7 readings, one readily concludes that there is experimental evidence of the development of symmetric distortional deformations at high load levels. It is worth noting that the recorded test images also show clearly the presence of visible (and fast growing) symmetric distortional deformations during the last loading steps, *i.e.*, in the vicinity of the column ultimate load.

5 COLUMN STRENGTH

In this section, one compares the column ultimate loads obtained experimentally (P_{exp}) with ultimate strength estimates yielded by the Direct Strength Method (DSM [6]) expressions prescribed in the North American specification [1] for columns failing globally ($P_{n.G}$) or due to local-global mode interaction ($P_{n.LG}$) – note that similar ultimate strength estimates could be determined by means of the "effective section method" included in the Brazilian code [2]. At this point, it is worth mentioning that the currently available DSM design expressions do not cover columns undergoing *L-D-G* interaction[3]. Table 2 provides tested column (i) measured cross-section areas (A) and lengths (L), (ii) squash loads ($P_y=Af_y$), (iii) experimental ultimate loads (P_{exp}), (iv) DSM ultimate strength estimates ($P_{n.G}$ and $P_{n.LG}$) and (v) the ultimate load ratios $P_{exp}/P_{n.G}$ and $P_{exp}/P_{n.LG}$ – the mean values, standard deviations and coefficients of variation of these last two sets of values are also presented. The observation of the results displayed in this table prompt the following comments:

(i) The $P_{n.G}$ estimates consistently overestimate the experimental ultimate loads by a large amount. Indeed, the minimum, maximum and mean values of the ratio $P_{exp}/P_{n.G}$ are *0.66*, *0.84* and *0.77*, respectively. This fact provides evidence of the ultimate strength erosion due to the *L-D-G* mode interaction phenomenon.

(ii) As for the $P_{n.LG}$ predictions, they still overestimate the experimental ultimate loads, but now by a smaller amount – the minimum, maximum and mean values of the ratio $P_{exp}/P_{n.LG}$ read *0.75*, *0.94* and *0.87*.

[3] In another paper included in these Proceedings, the authors address the development of a novel DSM design approach for cold-formed steel lipped channel columns affected by L-D-G mode interaction.

(a) (b)

Figure 4: Column (a) flexural-tortional deformed configuration and (b) local collapse mechanism.

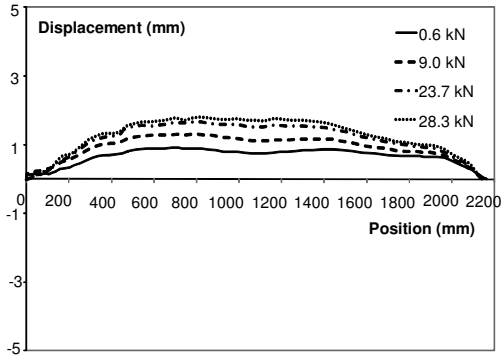

Figure 5: Displacement profiles measured by transducer DT8 along the column length.

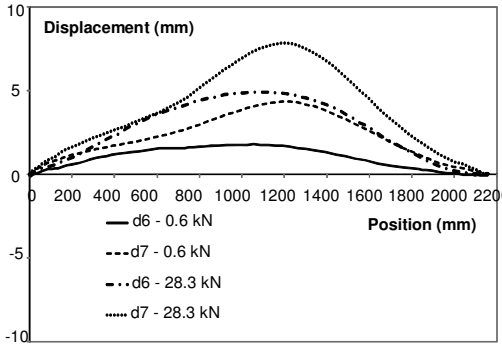

Figure 6: Displacement profiles measured by transducers DT6 and DT7 along the column length.

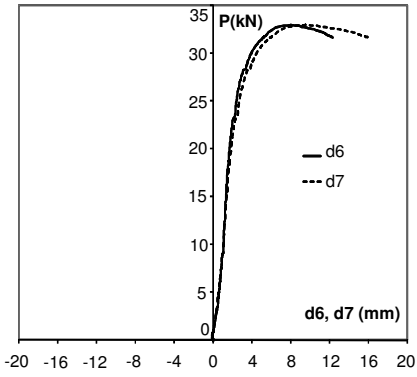

Figure 7: Measured displacements by transducers DT6 and DT7 at mid-height.

Figure 8 shows a comparison between the experimental loads and the ultimate strengths predicted by the two DSM expressions, for all the tested columns. This figure also includes the partial resistance factor γ, computed on the basis of the reliability equation prescribed by the Brazilian code [2],

$$\gamma = 1/\left[1.45 X_M\, X_F\, X_P \exp\left[-\beta_0 \left(V_M^2 + V_F^2 + C_P V_F^2 + 0.044\right)^{0.5}\right]\right] \quad (1)$$

where (i) X_M=*1.1*, X_F=*1.0* and X_P are the material, fabrication and load ratio P_{exp}/P_n mean values, respectively, (ii) β_0=2.5 is the target reliability value, and (iii) V_M=*0.1*, V_F=*0.05* and V_F are the material, fabrication and load ratio P_{exp}/P_n coefficients of variation, respectively. The results presented, which are based on (i) a live-to-dead load ratio (L_n/D_n) equal to *5* and (ii) the load combination $1.25D_n$+$1.5L_n$, lead to γ=*1.35* for the $P_{n.LG}$ estimates, a value that is above the regular one prescribed in the Brazilian code for cold-formed columns (γ

=1.20). In other words, the (DSM) $P_{n.LG}$ predictions do not meet the Brazilian code reliability requirement condition. Obviously, the performance of the $P_{exp}/P_{n.G}$ values is still significantly worse (γ*=1.51*).

Table 2: Column experimental ultimate loads and DSM ultimate strength estimates.

Column specimen	A (mm²)	L (cm)	P_{exp} (kN)	P_y (kN)	$P_{n.G}$ (kN)	$P_{n.LG}$ (kN)	$\frac{P_{exp}}{P_{n.G}}$	$\frac{P_{exp}}{P_{n.LG}}$	Config. at failure (experim.)
C1	273	2850	31.48	66.07	39.63	33.77	0.79	0.93	F-T
C2	272	2850	29.00	65.82	38.94	33.40	0.74	0.87	F-T
C3	274	2850	30.65	66.31	39.31	33.96	0.78	0.90	F-T
C4	238	2352	32.96	57.60	41.38	36.21	0.80	0.91	F-T
C5	238	2349	31.21	57.60	40.48	35.79	0.77	0.87	F-T
C6	238	2349	27.41	57.60	41.42	36.35	0.66	0.75	F-T
C7	223	2099	35.07	53.97	41.81	37.16	0.84	0.94	F-T
C8	221	2099	34.03	53.48	42.00	36.92	0.81	0.92	F-T
C9	203	1652	33.95	49.13	43.65	40.70	0.78	0.83	F-T
C10	204	1650	32.82	49.37	43.99	40.89	0.75	0.80	F-T
						Mean	0.77	0.87	
						Std. dev. σ	0.05	0.06	
						Coef. var. σ/mean	0.06	0.07	

F-T: flexural-torsional deformed configuration experimentally observed and recorded at failure.

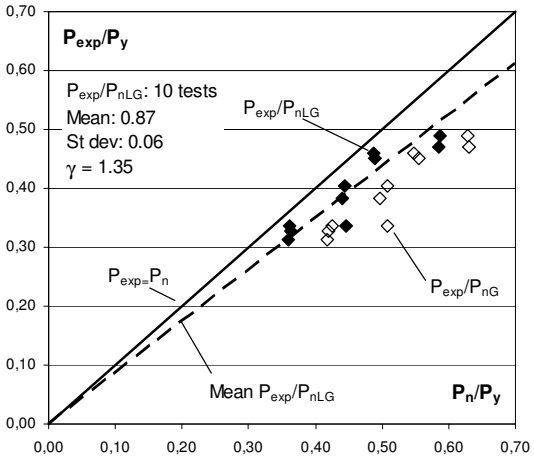

Figure 8: Comparison between experimental ultimate loads and DSM estimates $P_{n.G}$ and $P_{n.LG}$.

6 CONCLUDING REMARKS

The available results of an ongoing experimental investigation on fixed cold-formed steel lipped channel columns undergoing local-distortional-global mode interaction were reported – they concerned 10 column tests. After addressing the preliminary buckling analyses, which were performed by means of GBT-based analyses and made it possible to select appropriate cross-section dimensions and column lengths, the paper presented a detailed description of the experimental program carried out at COPPE/UFRJ. Next, the most relevant experimental results obtained during the tests were presented and discussed, namely column deformed configurations, collapse

mechanisms, displacement profiles and equilibrium paths. Finally, the paper closed with some considerations on the design of the columns investigated in this work, namely an experimental assessment of the application of the current DSM design expressions for global failures and collapses stemming from local-global interaction.

Out of the various conclusions drawn from the research work reported in this paper, the following ones deserve to be specially mentioned:

(i) All the tested columns exhibited clear flexural-torsional deformed configurations immediately before the collapse. The occurrence of local deformations was not detected, neither visually nor by means of the recorded displacement measurements. As for the symmetric distortional deformations, they were both captured by the displacement transducer readings and observed in the recorded test images. However, they were mainly visible during the last loading steps (close to the column ultimate load), when they developed quite fast.

(ii) In any case, the effects of the *L-D-G* interaction were clearly felt through a considerable erosion of the column ultimate strengths, with respect to the ultimate loads commonly expected from global failures.

(iii) Both the DSM $P_{n.G}$ (global failures) and $P_{n.LG}$ (collapses due to local-global interaction) ultimate strength estimates overestimated the experimental ultimate loads by a fair amount – no safe prediction was obtained. In addition, even the $P_{n.LG}$ estimates were found to exhibit a partial resistance factor that does not meet the reliability condition prescribed by the Brazilian code for cold-formed steel structures.

(iv) Further numerical and experimental work is required, in order to acquire more in-depth knowledge on a number of behavioural aspects associated with the mechanics of the *L-D-G* interaction.

REFERENCES

[1] AISI (American Iron and Steel Institute), *North American Specification for the Design of Cold-Formed Steel Members* (including an Appendix 1 on "Design of Cold-Formed Steel Structural Members using the Direct Strength Method), AISI S100-2007, 2007.

[2] ABNT (Associação Brasileira de Normas Técnicas – Brazil), *Design of Steel Structures with Cold-Formed Members*, ABNT-NBR14762, March 2010. (Portuguese)

[3] Kwon Y.B., Kim B.S. and Hancock G.J., "Compression tests of high strength cold-formed steel channels with buckling interaction", *Journal of Constructional Steel Research*, **65**(2), 278-289, 2009.

[4] Silvestre N., Camotim D. and Dinis P.B., "Direct strength prediction of lipped channel columns experiencing local-plate/distortional interaction", *Advanced Steel Construction - An International Journal*, **5**(1), 49-71, 2009.

[5] Young B., Camotim D. and Silvestre N., "Ultimate strength and design of lipped channel columns experiencing local/distortional mode interaction – part I: experimental investigation and part II: DSM design approach", *Proceedings of 6th International Conference on Advances in Steel Structures* (Hong Kong, 16-18/12), S.L. Chan (ed.), 460-469 + 470-479, 2009.

[6] Schafer B.W., "Review: the Direct Strength Method of cold-formed steel member design", *Journal of Constructional Steel Research*, **64**(7-8), 766-778, 2008.

[7] Dinis P.B. and Camotim D., "Post-buckling behaviour and strength of cold-formed steel lipped channel columns experiencing distortional/global interaction", *Computers & Stuctures*, accepted for publication, 2010.

[8] Dinis P.B. and Camotim, D., "Local/distortional/global buckling mode interaction in cold-formed steel lipped channel columns", *Proceedings of SSRC Annual Stability Conference* (Phoenix, 1-3/4), 295-323, 2009.

[9] Dinis P.B., Camotim D., Batista E.M. and Santos E.S., "Local/distortional/global mode coupling in fixed lipped channel columns: behaviour and strength". *Proceedings of 6th International Conference on Advances in Steel Structures* (Hong Kong, 16-18/12), S.L. Chan (ed.), , 2009.

[10] Santos E.S., *Strength and Stability Analysis of Cold-Formed Steel Members Affected by Local-Distortional-Global Buckling Mode Interaction*, M.Sc. Dissertation, Civil Engineering Program, COPPE, Federal University of Rio de Janeiro, 2010. (Portuguese)

[11] Bebiano R., Pina P., Silvestre N. and Camotim D., *GBTUL 1.0β – Buckling and Vibration Analysis of Thin-Walled Members*, DECivil/IST, Technical University of Lisbon, 2008. (http://www.civil.ist.utl.pt/gbt).